The Astrophysical Journal, 928:163 (7pp), 2022 April 1 https://doi.org/10.3847/1538-4357/ac573f

A Channel to Form Fast-spinning Black Hole–Neutron Star Binary Mergers as Multimessenger Sources

Rui-Chong Hu[1], Jin-Ping Zhu[2], Ying Qin[1,3], Bing Zhang[4,5], En-Wei Liang[1], and Yong Shao[6]
[1] Guangxi Key Laboratory for Relativistic Astrophysics, School of Physical Science and Technology, Guangxi University, Nanning 530004, People's Republic of China; yingqin2013@hotmail.com
[2] Department of Astronomy, School of Physics, Peking University, Beijing 100871, People's Republic of China; zhujp@pku.edu.cn
[3] Department of Physics, Anhui Normal University, Wuhu, Anhui 241000, People's Republic of China
[4] Nevada Center for Astrophysics, University of Nevada, Las Vegas, NV 89154, USA
[5] Department of Physics and Astronomy, University of Nevada, Las Vegas, NV 89154, USA
[6] Department of Astronomy, Nanjing University, Nanjing 210023, People's Republic of China
Received 2022 January 23; revised 2022 February 10; accepted 2022 February 17; published 2022 April 6

Abstract

After the successful detection of a gravitational-wave (GW) signal and its associated electromagnetic (EM) counterparts from GW170817, neutron star–black hole (NSBH) mergers have been highly expected to be the next type of multimessenger source. However, despite the detection of several NSBH merger candidates during the GW third observation run, no confirmed EM counterparts from these sources have been identified. The most plausible explanation is that these NSBH merger candidates were plunging events mainly because the primary black holes (BHs) had near-zero projected aligned spins based on GW observations. In view of the fact that neutron stars (NSs) can be easily tidally disrupted by BHs with high projected aligned spins, we study an evolution channel to form NSBH binaries with fast-spinning BHs, the properties of BH mass and spin, and their associated tidal disruption probability. We find that if the NSs are born first, the companion helium stars would be tidally spun up efficiently, and would thus finally form fast-spinning BHs. If BHs do not receive significant natal kicks at birth, these NSBH binaries that can merge within Hubble time would have BHs with projected aligned spins $\chi_z \gtrsim 0.8$ and, hence, can certainly allow tidal disruption to happen. Even if significant BH kicks are considered for a small fraction of NSBH binaries, the projected aligned spins of BHs are $\chi_z \gtrsim 0.2$. These systems can still be disrupted events unless the NSs are very massive. Thus, NS-first-born NSBH mergers would be promising multimessenger sources. We discuss various potential EM counterparts associated with these systems and their detectability in the upcoming fourth observation run.

Unified Astronomy Thesaurus concepts: Gravitational waves (678); Close binary stars (254); Black holes (162); Neutron stars (1108)

1. Introduction

Neutron star–black hole (NSBH) mergers are prime search targets for the ground-based gravitational-wave (GW) detectors, e.g., LIGO (LIGO Scientific Collaboration et al. 2015), Virgo (Acernese et al. 2015), and KAGRA (Aso et al. 2013). Recently, two high-confidence GW events (GW200105 and GW200115) were announced by the LIGO-Virgo-KAGRA (LVK) Collaboration, which was, for the first time, identified to come from mergers of NSBH binaries (Abbott et al. 2021a; Nitz et al. 2021). Furthermore, two lower mass-gap sources (GW190814 and GW200210_092254) that could either be from an NSBH or a binary black hole (BH), and several marginal NSBH candidates were discovered in GWs during the third observation run (O3) of LVK (Abbott et al. 2020b; The LIGO Scientific Collaboration et al. 2021a; Abbott et al. 2021b; The LIGO Scientific Collaboration et al. 2021b). The analysis of these NSBH candidates displayed that their effective inspiral spins could be near-zero or very low, suggesting that their primary BHs would plausibly have negligible projected spins aligned to the direction of the orbital angular momentum (abbreviated as projected aligned spins, hereafter). Among these candidates, only the BH component of GW200115 showed a nonzero BH spin with an apparent BH spin–orbit misalignment angle (Abbott et al. 2021a), which may require a strong natal kick for the BH or the neutron star (NS) (Fragione et al. 2021; Gompertz et al. 2022; Zhu 2021). Conversely, Mandel & Smith (2021) argued that GW200115 could potentially be a merger between a nonspinning BH and a typical mass of NS by reanalyzing its GW signal with the consideration of astrophysically motivated priors.

NSBH mergers have long been proposed to be progenitors of some fast-evolving electromagnetic (EM) counterparts, including short-duration gamma-ray bursts (sGRBs; Paczynski 1991; Narayan et al. 1992; Zhang 2018) and kilonovae (Li & Paczyński 1998; Metzger et al. 2010). As main GW sources of ground-based GW detectors, it was thus expected that the follow-up searches after GW triggers could help find out the associated EM signals of NSBH mergers. However, despite many efforts toward the follow-up observations, no confirmed EM counterpart candidate was identified (e.g., Coughlin et al. 2020a, 2020b; Gompertz et al. 2020b; Kasliwal et al. 2020; Page et al. 2020; Anand et al. 2021; Becerra et al. 2021). The tidal disruption probability of NSBH mergers and the brightness of EM signals depend on NS mass, NS equation of state (EOS), BH mass, and especially BH projected aligned spin (e.g., Kyutoku et al. 2015; Kawaguchi et al. 2016; Foucart et al. 2018; Barbieri et al. 2019; Zhu et al. 2020, 2021a, 2021b, 2021c;

Raaijmakers et al. 2021). Disrupted events associated with brighter EM signals tend to occur only if an NSBH binary has a low-mass NS component with a stiff EOS and a low-mass BH component with a high projected aligned spin. The most promising explanation for the lack of EM counterparts is that these NSBH candidates were plunging events without forming any bright EM signals, mainly due to their near-zero BH projected aligned spins (D'Orazio et al. 2022; Fragione 2021; Zhu et al. 2021b).

The most widely accepted formation channel for the majority of NSBH binaries in the universe is the classical common envelope (CE) scenario (e.g., Giacobbo & Mapelli 2018; Belczynski et al. 2020; Drozda et al. 2020; Broekgaarden et al. 2021; Shao & Li 2021). In this scenario, the immediate progenitor of an NSBH binary just after the CE phase is a close binary system, which consists of a compact object (NS or BH) and a helium star. On the one hand, if the firstborn compact object is a BH, its spin has been found to be negligible (Qin et al. 2018; Fuller & Ma 2019; Belczynski et al. 2020; Fuller & Lu 2022). This was supported by the finding of the near-zero distribution of BH spin in the O3 GW NSBH candidates (Zhu et al. 2021a), which implies that the NSs in these NSBH candidate systems may be directly plunged into the BHs. On the other hand, for a fraction of NSBH progenitor systems in which the NS was born first, the companion helium star can be spun up by the NS and finally form a BH with a high projected aligned spin. Since a fast-spinning BH can easily tidally disrupt the NS and produce bright EM signals (i.e., sGRBs and kilonovae), NSBH mergers formed via this formation channel can be potential multimessenger sources that allow us to discover their associated bright EM counterparts with a high probability after GW triggers (Zhu et al. 2021c). Furthermore, as studied recently by Román-Garza et al. (2021), core-collapse physics plays a critical role in the observability of the EM signals produced by NSBH mergers. In view of the lack of relevant research on the BH spin properties of this NS-first-born formation channel for NSBH mergers, we investigate this formation channel of NSBHs with fast-spinning BHs in detail and study their corresponding tidal disruption probability.

In this work, we investigate the detailed binary evolution process of forming fast-spinning BHs in NSBH binaries by taking into account the accretion feedback of the core-collapse processes, supernova (SN) kicks of newly formed BHs, and different NS EOSs. The main methods adopted in the stellar and binary evolution models are shown in Section 2. We then present in Section 3 our findings of NSBH mergers with and without natal kicks, respectively, along with their associated probability for tidal disruption. The multimessenger observational signatures of this channel are discussed in Section 4. Finally, our main conclusions are summarized in Section 5 with some discussion.

2. Methods

We use the release 15140 of the `MESA` stellar evolution code (Paxton et al. 2011, 2013, 2015, 2018, 2019) to perform all of the binary evolution calculations in this work. A metallicity of $Z = Z_{\odot}$, where the solar metallicity is $Z_{\odot} = 0.0142$ (Asplund et al. 2009), is adopted. We create single helium stars at the zero-age helium main sequence following the method in Qin et al. (2018) and then relax the created helium stars to reach the thermal equilibrium, where the He-burning luminosity just exceeds 99% of the total luminosity. We model convection using the mixing-length theory (Böhm-Vitense 1958) with a mixing-length parameter $\alpha = 1.93$. The Ledoux criterion is used to treat the boundaries of the convective zone, while we consider the step overshooting as an extension given by $\alpha_p = 0.1H_p$, where H_p is the pressure scale height at the Ledoux boundary limit. Semiconvection (Langer et al. 1983) with an efficiency parameter $\alpha = 1.0$ is also included in our model. The network of `approx12.net` is chosen for nucleosynthesis.

Stellar winds are modeled with the standard "`Dutch`" scheme, calibrated by multiplying with a scaling factor of 0.667 to match the recently updated modeling of helium stars' winds (Higgins et al. 2021). We model angular momentum transport and rotational mixing diffusive processes (Heger & Langer 2000), including the effects of Eddington–Sweet circulations, and the Goldreich–Schubert–Fricke instability, as well as secular and dynamical shear mixing. We adopt diffusive element mixing from these processes with an efficiency parameter of $f_c = 1/30$ (Chaboyer & Zahn 1992; Heger & Langer 2000). Mass transfer is modeled following the Kolb scheme (Kolb & Ritter 1990) and the implicit mass transfer method (Paxton et al. 2015) is adopted.

We model helium stars until the carbon depletion in the center. The baryonic remnant mass is calculated following the "delayed" supernova prescription in Fryer et al. (2012). As shown in Batta & Ramirez-Ruiz (2019), the newly formed BH might be unable to accrete all of the available stellar material. Therefore, in order to calculate the final mass and spin of the BH from the direct collapse, we follow the framework given in Batta & Ramirez-Ruiz (2019), which has already been implemented in a recent work (Bavera et al. 2020). The neutrino loss as in Zevin et al. (2020) is taken into account. Furthermore, the maximum NS mass is assumed to be $2.5\,M_{\odot}$ in this work.

BHs formed through direct collapse are considered to receive no mass loss and thus no natal kick (Belczynski et al. 2008). Recently, an estimation of the NSBH merger rate from the LIGO O3a run showed that negligible kicks imparted on the low-mass BHs is favored (Román-Garza et al. 2021). Consequently, calculation with no natal kick included is considered as our fiducial model. Additionally, we also take into account natal kicks onto BHs formed through direct collapse. We follow the parameterized recipes of Mandel & Müller (2020) to calculate the natal kicks of BHs. The binary properties just after the natal kick is given based on the framework of Kalogera (1996), Wong et al. (2012), and a recent work by Callister et al. (2021). For binaries surviving after the kick, we estimate the merger time given from Peters (1964) through GW emission, with the updated fitting formula for eccentricity in Mandel (2021).

3. Results

Here we present a parameter space study of the initial binary properties for a close binary system composed of a helium star and an NS. The parameters include the initial helium star masses and the initial orbital periods. We cover the helium star mass range 8–40 $M_{\odot}$, and the NS star mass range 1.2–2.5 $M_{\odot}$, as well as the orbital period from 0.2 to 2 days. We also take into account the natal kicks imparted onto BHs in the core-collapse models. We describe in detail our findings for the NSBH formation with and without natal kicks, respectively, along with their associated tidal disruption probability.

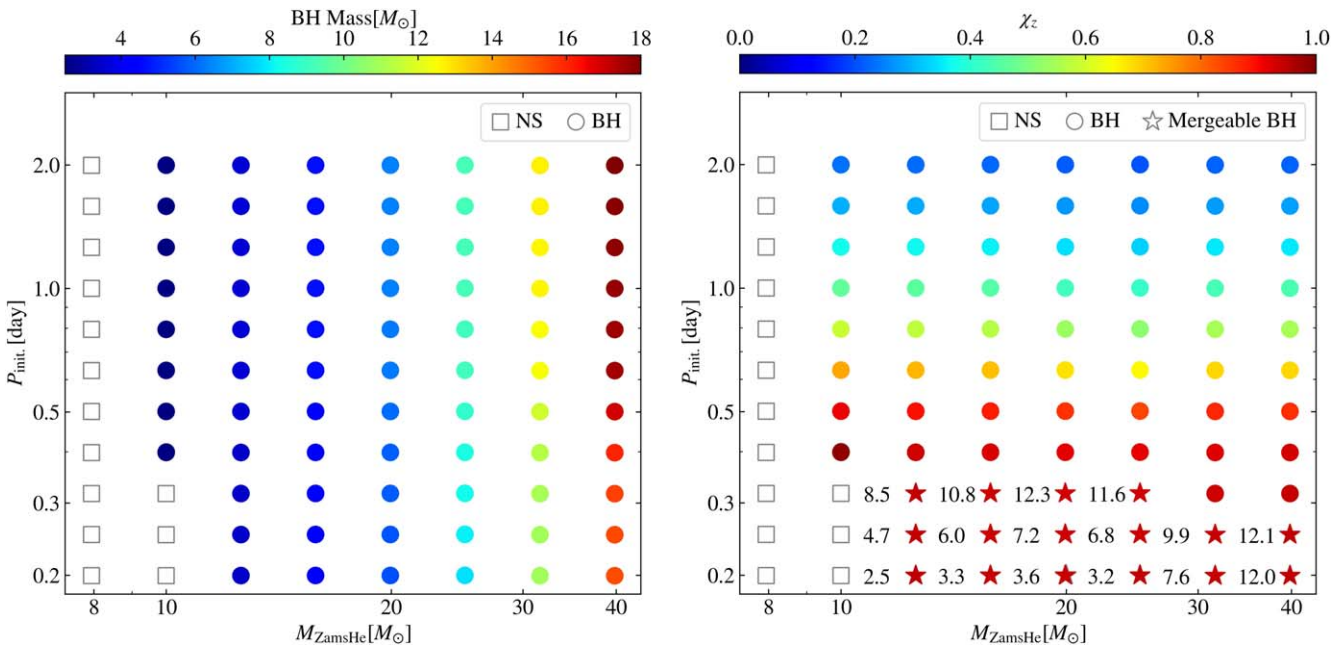

Figure 1. Left panel: BH mass (the color bar) as a function of the helium star initial mass and orbital period. The symbols represent different compact objects formed through the direct core collapse of the helium stars, i.e., squares for NSs and dots for BHs. Right panel: same as the left panel, but the color represents the BH projected aligned spins. The star symbols are marked with NSBH binaries that can be merged via GW emission within Hubble time. The numbers on the left side of the star symbols are the corresponding merger times in units of a billion years.

3.1. Fast-spinning BHs Originating from Tidal Spin-up in NSBH Binaries

Figure 1 presents various outcomes of the detailed binary evolution for helium stars at different initial masses orbiting around an NS of 1.4 $M_\odot$ in close orbits. We choose 2 days as the upper limit of the orbital period, beyond which tides are not important (Qin et al. 2018). We do not take into account the parameter space where the initial orbital periods are shorter than 0.2 days, as the binary would experience either initial overflow or dynamically unstable mass transfer. NSs with other masses have similar results, which are not shown in the paper.

First, we note from the left panel of Figure 1 that helium stars with an initial mass higher than 10 $M_\odot$ and an initial orbital period larger than ∼0.4 days collapse to form BHs. Furthermore, helium stars in tighter orbits tend to lose more mass due to rotationally enhanced mass loss (Heger & Langer 1998; Langer 1998). This is why we can see that helium stars in short orbits end up forming low-mass BHs. For low-mass (<10 $M_\odot$) helium stars, including a small fraction with initial orbital periods less than ∼0.3 days, NSs are formed instead. A further investigation of binary NS systems formed in our grid is postponed to a future work.

In the right panel of Figure 1, we show the magnitudes of the BH projected aligned spins for different initial binary properties. As shown in Qin et al. (2018), the spins of the resulting second-born BHs are exclusively dependent on the tidal interaction and stellar winds of the helium stars. For initial orbital periods considered in this gird, the BHs have the entire range of the spin from zero to a value allowed by maximally spinning. For more massive helium stars, their stellar winds are stronger, which widens the binaries and thus makes NSBHs undetectable for GW emission within Hubble time. Interestingly, we note that for helium stars with different initial masses, the BH projected aligned spins have a similar trend in decreasing magnitudes. After the formation of the second-born BH, the GW emission removes the orbital angular momentum of the NSBH, shrinks the orbit, and eventually leads to a merger of the two compact objects. The merger time is calculated as given in Peters (1964). It is worth noting that all NSBHs with merger times less than Hubble time have extremely fast spins. This finding is mainly attributed to the strong tidal force in close binaries. However, BHs formed through direct core collapse may receive SN kicks, which can change the direction of the BH spins and, hence, their projected aligned spins. The impact of SN kicks is discussed as follows.

3.2. Impact of SN Kicks on BH Projected Aligned Spins and the Probability of Merging NSBHs

The SN kicks imparted onto BHs are considered to cause a misalignment of the BH spin to the orbital angular momentum. In addition, the post-SN orbital separation and the eccentricity of the binary can also be modified. We briefly describe these calculations in the Appendix and more details can be found in Kalogera (1996), Wong et al. (2012), and Callister et al. (2021). Similar to Mandel & Müller (2020), kicks are drawn from a Gaussian distribution and we repeat 10^5 times to obtain the average value of the kick and also its associated angle θ. The corresponding averaged BH projected aligned spins ($\bar{\chi}_z$) are shown in the left panel of Figure 2. We note that $\bar{\chi}_z$ values are slightly less than those obtained assuming no kicks (see the right panel of Figure 1). This is because the SN kicks we apply to the BHs are typically small (see the red line for BH kicks in Figure 4 of Mandel & Smith 2021). Accordingly, we then obtain on average a small misalignment for BH spins.

Let us see how kicks change the fraction of merging NSBHs. As shown in the right panel of Figure 2, with the post-SN-explosion binary properties updated, for each initial system we can then calculate the fraction of the post-SN-explosion NSBH systems that can survive and merge within Hubble time. The BH masses of these systems against their BH projected aligned

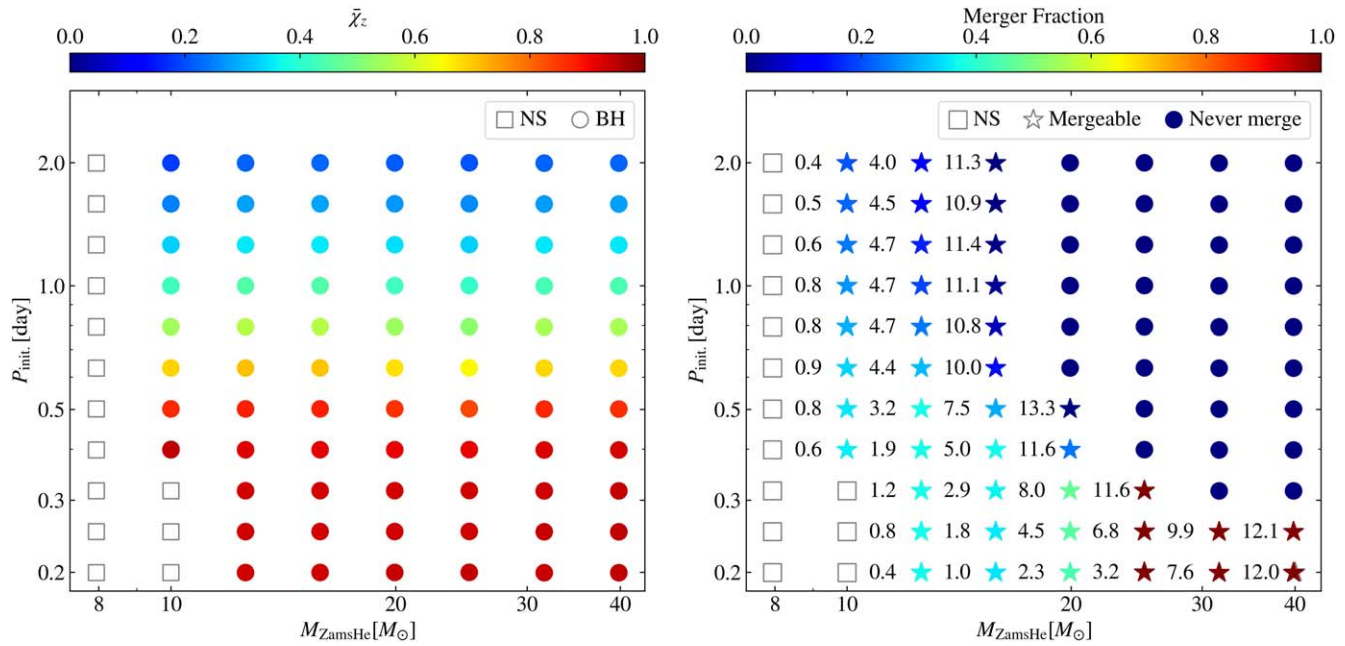

Figure 2. Left panel: similar to the left panel in Figure 1, but with SN kicks included. Right panel: the color represents the fraction of NSBH binaries that can be merged within Hubble time with SN kicks considered. The numbers on the left side of the star symbols are the medians of the corresponding merger times in units of a billion years that are less than Hubble time. Dark-blue dots: NSBH binaries that never merge within Hubble time.

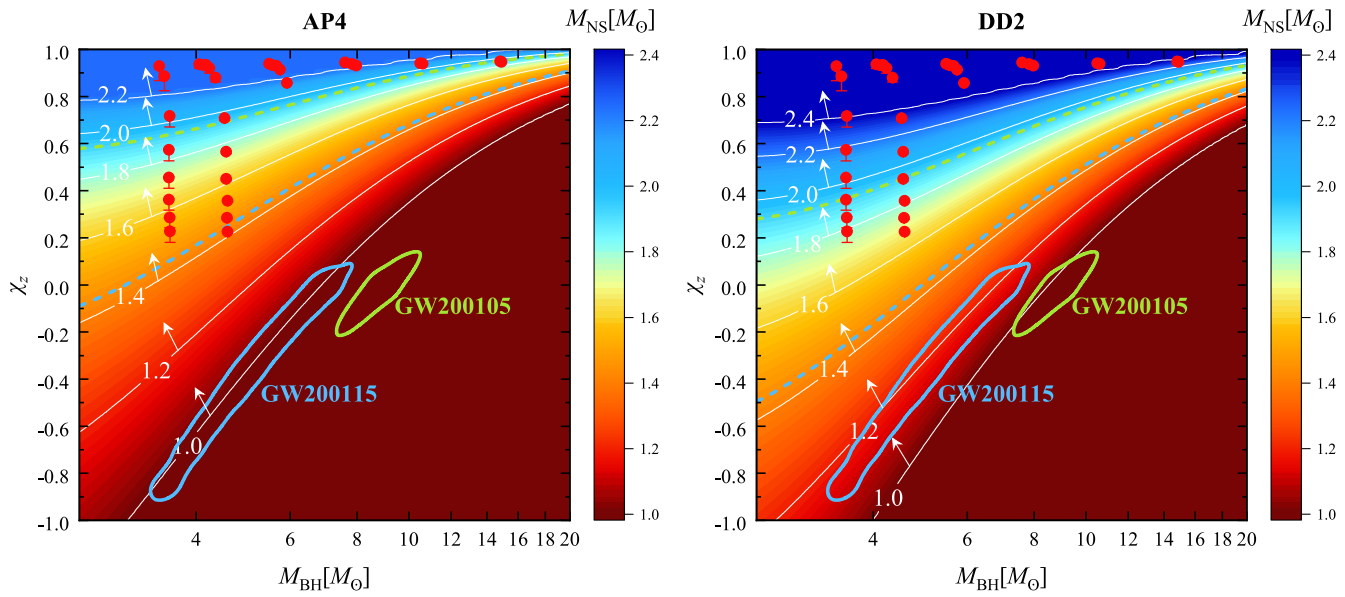

Figure 3. The median and 90% confidence interval of BH projected aligned spin vs. BH mass from the grid of calculations for those merger events within Hubble time used to produce Figure 2 (red circles), and the parameter space for NSBH merger systems to allow tidal disruption of the NS by the BH. Two EOSs, i.e., AP4 (left panel) and DD2 (right panel), are considered. We mark several values of the NS mass from $M_{\rm NS} = 1\,M_\odot$ to $M_{\rm NS} = 2.2\,M_\odot$ for AP4 ($M_{\rm NS} = 2.4\,M_\odot$ for DD2) as solid lines in each panel. For a specific $M_{\rm NS}$, the NSBH mergers with BH mass and BH projected aligned spin located at the top left parameter space (denoted by the direction of the arrows) can allow tidal disruptions to occur. For GW200105 (green) and GW200115 (blue), the 90% credible posterior distributions (colored solid lines) of the parameters obtained from Abbott et al. (2021a) are displayed, respectively. Corresponding median values of $M_{\rm NS}$ for these two sources are marked as dashed lines. Both GW200105 and GW200115, which are believed to form via the BH-first-born formation scenario (Broekgaarden & Berger 2021; Kinugawa et al. 2022), are most likely plunging events.

spins are presented in Figure 3. As the kick is considered, massive BHs with $M_{\rm BH} \gtrsim 7.6\,M_\odot$ do not experience natal kicks (see the last three columns from the right side) as they are heavier than the carbon–oxygen core of their progenitors at the pre-SN state. Some NSBH binaries with relatively low spins, which cannot merge in a wide orbit, can instead merge within Hubble time caused by the SN kicks. However, the merger fraction deceases since the systems have lower-mass BHs with lower projected aligned spins. More specifically, as shown in Figure 3, BHs with $M_{\rm BH} \lesssim 5\,M_\odot$ have a wide range of projected aligned spins χ_z from $\sim$0.2 to $\sim$1.0, while more massive BHs are found to be extremely spinning, i.e., $\chi_z \gtrsim 0.8$.

The firstborn BHs in NSBH mergers are expected to have near-zero spin distributions (e.g., Qin et al. 2018; Belczynski et al. 2020). Broekgaarden & Berger (2021) and Kinugawa et al. (2022) suggested that GW200105 and GW200115 are

expected to be formed via the classical BH-first-born isolated formation channel. Their posterior distributions of BH projected aligned spin versus BH mass from Abbott et al. (2021a) are plotted in Figure 3. It is clear that the distributions of the BH projected aligned spin for GW200105 and GW200115 are quite different from our calculated distributions for NS-first-born NSBH mergers.

3.3. Tidal Disruption Probability

The tidal disruption probability of NSBH mergers is determined by NS mass, NS EOS, BH mass, and BH projected aligned spin. It remains unclear whether NSs can accrete angular momentum and thus be spun up during the CE evolution or not (Barkov & Komissarov 2011). Chattopadhyay et al. (2021) recently predicted that NSs in NS-first-born NSBH mergers can have spins from a few milliseconds to a few tens of seconds, which corresponds to dimensional spins with a range of $\chi_{\rm NS} < 0.05$. Such nonnegligible NS spins are still too weak to affect the tidal disruption of NSBH mergers, so that the NS spins can be ignored when we calculate tidal disruption probability. By considering two representative EOSs, i.e., AP4 (Akmal & Pandharipande 1997) and DD2 (Typel et al. 2010), in which AP4 is one of the most likely EOSs while DD2 is one of the stiffest EOSs constrained by GW170817 (Abbott et al. 2018, 2019), the parameter space where the NS can be tidally disrupted using the formula from Foucart et al. (2018) is shown in Figure 3. An NSBH binary system that has a lower-mass NS with a stiffer EOS and a lower-mass BH with a higher projected aligned spin can more easily make tidal disruption. The Tolman–Oppenheimer–Volkov (TOV) masses for the EOSs of AP4 and DD2 are $M_{\rm TOV} = 2.22\,M_\odot$ and $2.42\,M_\odot$, respectively. On one hand, for almost all of the parameter space of the NS mass, Figure 3 reveals that NSBH mergers formed via the NS-first-born formation scenario should be disrupted events if the remnant BHs are heavier than $\sim 5\ M_\odot$. Furthermore, for the BH mass located in the range of $M_{\rm BH} \lesssim 5\,M_\odot$, NSBH mergers whose BH projected aligned spins are $\chi_z > 0.8$ are expected to make tidal disruption as shown in Figure 3. On the other hand, some mergers of NSBH binaries with relatively low BH projected aligned spins (i.e., $\chi_z \lesssim 0.8$) caused by the impact of SN kicks on low-mass BH components could still be plunging events, if the mass of the NS companions is $M_{\rm NS} \gtrsim 1.5\,M_\odot$ ($M_{\rm NS} \gtrsim 1.7\,M_\odot$) with the adoption of an EOS of AP4 (DD2). However, since the fraction of NSBH binaries with low BH projected aligned spins that can merge within Hubble time after the SN kick is limited as discussed in Section 3.2, plunging events may account for only a small part of NSBH mergers formed via the NS-first-born formation scenario. Therefore, regardless of the EOS we choose, it is expected that most NSs can be tidally disrupted by the BHs in NS-first-born NSBH merger systems and they would be plausible multimessenger sources, which may be discovered in the future.

4. Observational Signatures

4.1. Multimessenger Signals

In Section 3.3, we showed that most of NS-first-born NSBH mergers can easily make tidal disruption. Disrupted NSBH mergers are believed to drive some bright EM counterparts. After an NSBH merger, there might be a pair of relativistic jets launched along the polar axis by the accreting remnant BH via the Blandford–Znajek effect (Blandford & Znajek 1977; Gompertz et al. 2020a), which can power an sGRB and its broadband afterglow emission as the jet interacts with the interstellar medium. The radioactive decays of the rapid neutron-capture-formed heavy nuclei can effectively heat the ejected materials in the dynamic ejecta or the wind outflows launched from the disk around the remnant BH, which would power the fast-evolving kilonova emission (e.g., Kawaguchi et al. 2016; Barbieri et al. 2019; Zhu et al. 2020; Darbha et al. 2021). The brightness of the emission may be further enhanced by the energy injection from the central engine (e.g., Ma et al. 2018; Qi et al. 2022). Sridhar et al. (2021) presented that some radio emissions beamed along the equatorial plane of an NSBH merger.

In the fourth observing run (O4), the number of detected NSBH GWs is believed to increase significantly (e.g., Abbott et al. 2020a; Zhu et al. 2021c). A higher accuracy in both localization and distance measurement by the GW observations is expected, making the post-GW-trigger follow-up search observations more efficient. Furthermore, during the same GW period, several more powerful telescopes, e.g., the Space Variable Objects Monitor (Wei et al. 2016) in gamma-rays, the Einstein Probe (Yuan et al. 2016) in X-rays, the Large Synoptic Survey Telescope (LSST Science Collaboration et al. 2009), and the Wide-field Infrared Transient Explorer (Frostig et al. 2022) in optical-infrared bands, will start to operate and join the GW follow-up observational campaigns. It is possible that multi-messenger signals from NSBH mergers, especially for NS-first-born NSBH mergers, could be discovered in the forthcoming O4.

4.2. A Possible Connection between Long-duration and Short-duration GRBs

One interesting inference from this channel is that there could be a common progenitor system for a small fraction of long-duration GRBs (lGRBs) and sGRBs. As shown in Section 3, the resulting BHs in close binaries are found to be highly spinning due to tidal spin-up. Such a fast-spinning BH can in principle launch a relativistic jet and produce an lGRB through the Blandford–Znajek mechanism (Blandford & Znajek 1977) during the formation of the second-born BH. After the formation of the BH, the NSBH binary would merge long time later after losing orbital energy and angular momentum due to GW emission. Eventually, an sGRB may be produced at the merger.

We show for each NSBH system the merger time, namely the time delay between the lGRB and the following sGRB, on the left side of the symbol in the right panel of Figure 1. The time delay varies from a few tens to hundreds of billions of years. When the SN kicks imparted onto the newly formed BHs are considered, the average merger time[7] drops by roughly 1–2 orders of magnitude (see the right panel of Figure 2). In any case, the delay time is too long and it is impossible to directly test the existence of both an lGRB and an sGRB from the same progenitor system observationally. One possible approach to test this scenario is through host galaxy studies. It has been well established that lGRBs and sGRBs have statistically very different host properties (e.g., Fruchter et al. 2006; Fong et al. 2010; Li et al. 2016). Comparing the host properties with the consideration of galaxy evolution in the timescale of the delay between the SN explosion and merger may offer some clues. This is beyond the scope of this paper.

[7] We adopt the median of the merger time in 10^5 times drawings as the average merger time. We exclude the systems that are disrupted or whose merger times are beyond Hubble time.

5. Conclusions and Discussion

In this work, we first present a detailed binary evolution modeling of the formation of NSBH systems, concentrating on a special channel in which NSs are first formed and BHs are born with high natal spins. With this formation scenario considered, we explore the tidal disruption probability of NSBH mergers, taking into account the impact of accretion feedback of direct core-collapse modeling on the mass and spin of the newly formed BHs, SN kicks, and different NS EOSs. We find that these NSBH mergers produce BHs with extremely high natal spins. With no natal kicks for BHs, we note that NSBH binaries that can merge within Hubble time would have BHs with the projected aligned spins $\chi_z \gtrsim 0.8$, and therefore can definitely have tidal disruption of the NSs at the merger. On the other hand, when natal kicks are taken into account, BHs with $M_{\rm BH} \lesssim 5\,M_\odot$ and with projected aligned spins χ_z down to 0.2 (see the right panel of Figure 2) can still merge with an NS within Hubble time, but with a low probability. These systems can still be disrupted events and produce bright EM signals unless the NSs are very massive.

Metallicity plays a critical role in evolving binary stars. First, stars at metal-poor environments where the stellar winds are weaker (Vink et al. 2001) lose less mass and thus form heavier BHs. Second, at a lower metallicity, the winds take less angular momentum away from the system, which tends to keep the binaries closer (see Figures 7 and 8 for final orbital periods at lower metallicities in Qin et al. 2018) and shortens the delay time. Given the solar metallicity considered in this work, our results are probably more suitable to environments like our Galaxy. The extension of our current grids with many other metallicities (especially lower metallicities) has been considered for our study in the near future.

Román-Garza et al. (2021) claimed that the fraction of NS-first-born systems with different SN engines is $\lesssim$10% (see also Kinugawa et al. 2022). Recent population synthesis studies (Broekgaarden et al. 2021; Chattopadhyay et al. 2021) showed that the fraction of NS-first-born NSBH binaries in total galactic NSBH binaries highly depends on the variations of binary population synthesis assumptions. Their simulations revealed that NS-first-born NSBHs, with a fraction of $\lesssim$20%, are at least less than 1 order of magnitude—but can be as high as several orders of magnitude—more infrequent than BH-first-born NSBHs when considering different variations in their population synthesis models (see Table 4 in Chattopadhyay et al. 2021). The event rate and system parameter distribution for NS-first-born NSBH mergers are subject to further studies in the future.

Very recently, Olsen et al. (2022) reported a marginal candidate, GW190920_113516, whose secondary could be a heavy NS. With an effective inspiral spin of $\chi_{\rm eff} = 0.60^{+0.26}_{-0.07}$, this event could be a potential NSBH merger where the NS was born first. With the upgrade of GW observatories and the update of large survey telescopes, it is foreseen that one may detect high-confidence GW signals with associated EM counterparts from NSBH mergers, especially for NS-first-born NSBH mergers, in the near future of this GW-led multi-messenger era.

Y.Q. acknowledges the support of the Doctoral research start-up funding from Anhui Normal University and of the Key Laboratory for Relativistic Astrophysics in Guangxi University. E.W.L. is supported by the National Natural Science Foundation of China (grant Nos. 12133003, U1731239) and the Guangxi Science Foundation (grant No. AD17129006). This work is supported by the National Natural Science Foundation of China (grant Nos. 12192220, 12192221) and by the Natural Science Foundation of Universities in Anhui Province (grant No. KJ2021A0106). All figures were made with the free Python module Matplotlib (Hunter 2007).

The inlists and input files to reproduce our simulations and associated data products are available at https://doi.org/10.5281/zenodo.6033230.

Appendix

Our implementation for natal kicks, imparted on the newly formed BH, is based on the framework of Kalogera (1996), Wong et al. (2012), and a recent work in Callister et al. (2021). Following the prescription in Mandel & Müller (2020), the mean natal kick for BHs is

$$\mu_{\rm kick} = v_{\rm BH}\frac{\max\left(M_{\rm CO} - M_{\rm BH}, 0\right)}{M_{\rm BH}}, \tag{1}$$

where $v_{\rm BH}$ is the BH scaling prefactor and $M_{\rm CO}$ is the carbon–oxygen core (CO core) mass, respectively. We adopt $v_{\rm BH} = 200\,{\rm km\,s^{-1}}$ as suggested in Mandel & Müller (2020). We also add an additional component drawn from a Gaussian distribution with the standard deviation $0.3\mu_{\rm kick}$.

We update the semimajor axis and the eccentricity of the binary after the supernova (SN) kick following Kalogera (1996):

$$a_f = G(M_{\rm NS} + M_{\rm BH})\left[\frac{2G(M_{\rm NS} + M_{\rm BH})}{a_i} - v_{\rm kick}^2 - v_{\rm orb}^2 - 2v_{\rm kick,y}v_{\rm orb}\right]^{-1} \tag{2}$$

and

$$1 - e^2 = \frac{(v_{\rm kick,y}^2 + v_{\rm kick,z}^2 + v_{\rm orb}^2 + 2v_{\rm kick,y}v_{\rm orb})a_i^2}{G(M_{\rm NS} + M_{\rm BH})a_f} \tag{3}$$

where G is Newton's constant, a_i and a_f are the pre- and post-SN semimajor axes, and $v_{{\rm kick},i}$ represents the ith component of the kick velocity $\mathbf{v}_{\rm kick}$. Here $v_{\rm orb}$, the pre-SN orbital velocity of the BH progenitor relative to its companion (NS), is given (Wong et al. 2012) by

$$v_{\rm orb}^2 = G(M_{\rm NS} + M_{\rm pre-SN})\left(\frac{2}{r} - \frac{1}{a_i}\right), \tag{4}$$

where r is the orbital separation between the BH progenitor and its companion at the pre-SN stage and $M_{\rm pre-SN}$ ($M_{\rm He}$ at the pre-SN phase) is the mass of the BH progenitor just prior to the SN explosion. The expression of r is given in Equation (15) in Wong et al. (2012).

Following the same assumption (Kalogera 1996) that the explosion is instantaneous, r remains unchanged. As a result, the angle θ between the pre- and post-SN orbital planes is determined by

$$\cos\theta = \frac{v_{\rm kick,y} + v_{\rm orb}}{[(v_{\rm kick,y} + v_{\rm orb})^2 + v_{\rm kick,z}^2]^{1/2}}. \tag{5}$$

If the natal kick is too strong, the binary after the supernova explosion will be disrupted. As shown in Callister et al. (2021),

the binary is disrupted when

$$\beta < \frac{1}{2} + \frac{v_{\rm kick}^2}{2v_{\rm orb}^2} + \frac{\mathbf{v}_{\rm kick}\cdot\mathbf{v}_{\rm orb}}{v_{\rm orb}^2}, \quad (6)$$

where β is defined in Equation (7) in Kalogera (1996) as the pre-SN-to-post-SN ratio of the binary's total mass. For binaries surviving after the SN kicks, we can calculate the merger time via gravitational-wave emission (Mandel 2021), i.e.,

$$T_{\rm merger} = \frac{5}{256}\frac{c^5 a_f^4}{G^3(M_{\rm NS}+M_{\rm BH})^2 m_r} T(e), \quad (7)$$

where c is the speed of light, m_r is the binary's reduced mass, and the function $T(e)$ is given by

$$T(e) = (1 + 0.27e^{10} + 0.33e^{20} + 0.2e^{1000})(1-e^2)^{7/2}. \quad (8)$$

ORCID iDs

Rui-Chong Hu https://orcid.org/0000-0002-6442-7850
Jin-Ping Zhu https://orcid.org/0000-0002-9195-4904
Ying Qin https://orcid.org/0000-0002-2956-8367
Bing Zhang https://orcid.org/0000-0002-9725-2524
En-Wei Liang https://orcid.org/0000-0002-7044-733X
Yong Shao https://orcid.org/0000-0003-2506-6906

References

Abbott, B. P., Abbott, R., Abbott, T. D., et al. 2018, PhRvL, 121, 161101
Abbott, B. P., Abbott, R., Abbott, T. D., et al. 2019, PhRvX, 9, 011001
Abbott, B. P., Abbott, R., Abbott, T. D., et al. 2020a, LRR, 23, 3
Abbott, R., Abbott, T. D., Abraham, S., et al. 2020b, ApJL, 896, L44
Abbott, R., Abbott, T. D., Abraham, S., et al. 2021a, ApJL, 915, L5
Abbott, R., Abbott, T. D., Abraham, S., et al. 2021b, PhRvX, 11, 021053
Acernese, F., Agathos, M., Agatsuma, K., et al. 2015, CQGra, 32, 024001
Akmal, A., & Pandharipande, V. R. 1997, PhRvC, 56, 2261
Anand, S., Coughlin, M. W., Kasliwal, M. M., et al. 2021, NatAs, 5, 46
Aso, Y., Michimura, Y., Somiya, K., et al. 2013, PhRvD, 88, 043007
Asplund, M., Grevesse, N., Sauval, A. J., & Scott, P. 2009, ARA&A, 47, 481
Barbieri, C., Salafia, O. S., Perego, A., Colpi, M., & Ghirlanda, G. 2019, A&A, 625, A152
Barkov, M. V., & Komissarov, S. S. 2011, MNRAS, 415, 944
Batta, A., & Ramirez-Ruiz, E. 2019, arXiv:1904.04835
Bavera, S. S., Fragos, T., Qin, Y., et al. 2020, A&A, 635, A97
Becerra, R. L., Dichiara, S., Watson, A. M., et al. 2021, MNRAS, 507, 1401
Belczynski, K., Taam, R. E., Rantsiou, E., & van der Sluys, M. 2008, ApJ, 682, 474
Belczynski, K., Klencki, J., Fields, C. E., et al. 2020, A&A, 636, A104
Blandford, R. D., & Znajek, R. L. 1977, MNRAS, 179, 433
Böhm-Vitense, E. 1958, ZAp, 46, 108
Broekgaarden, F. S., & Berger, E. 2021, ApJL, 920, L13
Broekgaarden, F. S., Berger, E., Neijssel, C. J., et al. 2021, MNRAS, 508, 5028
Callister, T. A., Farr, W. M., & Renzo, M. 2021, ApJ, 920, 157
Chaboyer, B., & Zahn, J. P. 1992, A&A, 253, 173
Chattopadhyay, D., Stevenson, S., Hurley, J. R., Bailes, M., & Broekgaarden, F. 2021, MNRAS, 504, 3682
Coughlin, M. W., Dietrich, T., Antier, S., et al. 2020a, MNRAS, 492, 863
Coughlin, M. W., Dietrich, T., Antier, S., et al. 2020b, MNRAS, 497, 1181
Darbha, S., Kasen, D., Foucart, F., & Price, D. J. 2021, ApJ, 915, 69
D'Orazio, D. J., Haiman, Z., Levin, J., Samsing, J., & Vigna-Gomez, A. 2022, ApJ, 927, 56
Drozda, P., Belczynski, K., O'Shaughnessy, R., Bulik, T., & Fryer, C. L. 2020, arXiv:2009.06655
Fong, W., Berger, E., & Fox, D. B. 2010, ApJ, 708, 9
Foucart, F., Hinderer, T., & Nissanke, S. 2018, PhRvD, 98, 081501
Fragione, G. 2021, ApJL, 923, L2
Fragione, G., Loeb, A., & Rasio, F. A. 2021, ApJL, 918, L38
Frostig, D., Biscoveanu, S., Mo, G., et al. 2022, ApJ, 926, 152
Fruchter, A. S., Levan, A. J., Strolger, L., et al. 2006, Natur, 441, 463
Fryer, C. L., Belczynski, K., Wiktorowicz, G., et al. 2012, ApJ, 749, 91
Fuller, J., & Lu, W. 2022, MNRAS, 511, 3951
Fuller, J., & Ma, L. 2019, ApJL, 881, L1
Giacobbo, N., & Mapelli, M. 2018, MNRAS, 480, 2011
Gompertz, B. P., Cutter, R., Steeghs, D., et al. 2020b, MNRAS, 497, 726
Gompertz, B. P., Levan, A. J., & Tanvir, N. R. 2020a, ApJ, 895, 58
Gompertz, B. P., Nicholl, M., Schmidt, P., Pratten, G., & Vecchio, A. 2022, MNRAS, 511, 1454
Heger, A., & Langer, N. 1998, A&A, 334, 210
Heger, A., & Langer, N. 2000, ApJ, 544, 1016
Higgins, E. R., Sander, A. A. C., Vink, J. S., & Hirschi, R. 2021, MNRAS, 505, 4874
Hunter, J. D. 2007, CSE, 9, 90
Kalogera, V. 1996, ApJ, 471, 352
Kasliwal, M. M., Anand, S., Ahumada, T., et al. 2020, ApJ, 905, 145
Kawaguchi, K., Kyutoku, K., Shibata, M., & Tanaka, M. 2016, ApJ, 825, 52
Kinugawa, T., Nakamura, T., & Nakano, H. 2022, arXiv:2201.06713
Kolb, U., & Ritter, H. 1990, A&A, 236, 385
Kyutoku, K., Ioka, K., Okawa, H., Shibata, M., & Taniguchi, K. 2015, PhRvD, 92, 044028
Langer, N. 1998, A&A, 329, 551
Langer, N., Fricke, K. J., & Sugimoto, D. 1983, A&A, 126, 207
Li, L.-X., & Paczyński, B. 1998, ApJL, 507, L59
Li, Y., Zhang, B., & Lü, H.-J. 2016, ApJS, 227, 7
LIGO Scientific Collaboration, Aasi, J., Abbott, B. P., et al. 2015, CQGra, 32, 074001
LSST Science Collaboration, Abell, P. A., Allison, J., et al. 2009, arXiv:0912.0201
Ma, S.-B., Lei, W.-H., Gao, H., et al. 2018, ApJL, 852, L5
Mandel, I. 2021, RNAAS, 5, 223
Mandel, I., & Müller, B. 2020, MNRAS, 499, 3214
Mandel, I., & Smith, R. J. E. 2021, ApJL, 922, L14
Metzger, B. D., Martínez-Pinedo, G., Darbha, S., et al. 2010, MNRAS, 406, 2650
Narayan, R., Paczynski, B., & Piran, T. 1992, ApJL, 395, L83
Nitz, A. H., Kumar, S., Wang, Y.-F., et al. 2021, arXiv:2112.06878
Olsen, S., Venumadhav, T., Mushkin, J., et al. 2022, arXiv:2201.02252
Paczynski, B. 1991, AcA, 41, 257
Page, K. L., Evans, P. A., Tohuvavohu, A., et al. 2020, MNRAS, 499, 3459
Paxton, B., Bildsten, L., Dotter, A., et al. 2011, ApJS, 192, 3
Paxton, B., Cantiello, M., Arras, P., et al. 2013, ApJS, 208, 4
Paxton, B., Marchant, P., Schwab, J., et al. 2015, ApJS, 220, 15
Paxton, B., Schwab, J., Bauer, E. B., et al. 2018, ApJS, 234, 34
Paxton, B., Smolec, R., Schwab, J., et al. 2019, ApJS, 243, 10
Peters, P. C. 1964, PhRv, 136, 1224
Qi, Y.-Q., Liu, T., Huang, B.-Q., Wei, Y.-F., & Bu, D.-F. 2022, ApJ, 925, 43
Qin, Y., Fragos, T., Meynet, G., et al. 2018, A&A, 616, A28
Raaijmakers, G., Nissanke, S., Foucart, F., et al. 2021, ApJ, 922, 269
Román-Garza, J., Bavera, S. S., Fragos, T., et al. 2021, ApJL, 912, L23
Shao, Y., & Li, X.-D. 2021, ApJ, 920, 81
Sridhar, N., Zrake, J., Metzger, B. D., Sironi, L., & Giannios, D. 2021, MNRAS, 501, 3184
The LIGO Scientific Collaboration, the Virgo Collaboration, Abbott, R., et al. 2021a, arXiv:2108.01045
The LIGO Scientific Collaboration, the Virgo Collaboration, the KAGRA Collaboration, et al 2021b, arXiv:2111.03606
Typel, S., Röpke, G., Klähn, T., Blaschke, D., & Wolter, H. H. 2010, PhRvC, 81, 015803
Vink, J. S., de Koter, A., & Lamers, H. J. G. L. M. 2001, A&A, 369, 574
Wei, J., Cordier, B., Antier, S., et al. 2016, arXiv:1610.06892
Wong, T.-W., Valsecchi, F., Fragos, T., & Kalogera, V. 2012, ApJ, 747, 111
Yuan, W., Amati, L., Cannizzo, J. K., et al. 2016, SSRv, 202, 235
Zevin, M., Spera, M., Berry, C. P. L., & Kalogera, V. 2020, ApJL, 899, L1
Zhang, B. 2018, The Physics of Gamma-Ray Bursts (Cambridge: Cambridge Univ. Press)
Zhu, J.-P., Wu, S., Qin, Y., et al. 2021a, arXiv:2112.02605
Zhu, J.-P., Wu, S., Yang, Y.-P., et al. 2021b, ApJ, 921, 156
Zhu, J.-P., Wu, S., Yang, Y.-P., et al. 2021c, ApJ, 917, 24
Zhu, J.-P., Yang, Y.-P., Liu, L.-D., et al. 2020, ApJ, 897, 20
Zhu, X.-J. 2021, ApJL, 920, L20